Oxygen Reduction Reaction Catalyst

Field of the Invention

The present invention relates to catalysts for use in, inter alia, fuel cells and metal_/air batteries. In particular, the invention relates to catalysts for the oxygen reduction reaction in fuel cells, and most particularly to non-metallic catalysts for the oxygen reduction reactions in fuel cells. The invention also relates to fuel cells comprising said catalysts and to the use of said catalysts in the catalytic reduction of oxygen at the cathode of fuel cells.

Background

Energetic resources which offer a viable alternative to the burning of fossil fuels are of great interest at present in view of the increasing worldwide energy demand and the environmental concerns associated with fossil fuels such as gasoline and diesel. Fuel cell technology, which relies on the conversion of chemical energy to electricity through electrocatalytic reactions, has received a great deal of attention in this respect as it offers a high-efficiency, environmentally benign energy source which is also well suited to transportation and mobile applications.

A fuel cell is an electrochemical device which oxidises fuel at the anode and reduces oxygen from the air at the cathode. In most fuel cells the efficiency of the oxygen reduction reaction at the cathode is a crucial factor in the performance of the cell and for this reason this reaction is usually catalysed using the most efficient methods known. This is typically by employing catalysts such as platinum group metals and their alloys.

Commonly, an ion exchange membrane is positioned between the anode and the cathode to form a proton-exchange membrane fuel cell (PEMFC). Although highly efficient, the rate of the oxygen reduction reaction (ORR) of the platinum (Pt) catalyst remains too slow to allow PEMFCs to become successful alternatives to fossil fuels in most markets. Added to this, are factors that can reduce the lifetime of PEMFCs, including: (1) platinum-particle dissolution and sintering, (2) carbon

support corrosion, and (3) CO deactivation of Pt surface area in the cathode. At present the ORR rate at the cathode is 6 orders of magnitude slower than that of its anodic counterpart, leading to the necessity of using increased (0.4 $mgPt/cm^2$) loadings of commercially optimized Pt/carbon black cathode catalysts. In commercial applications such as transport, this catalyst can cost several thousands of dollars per vehicle. It is estimated that an approximately five-fold reduction of the amount of Pt (platinum-loading) in current PEMFC stacks is needed to meet the cost requirements for large-scale auto-motive applications. In order for the large-scale practical application of fuel cells to be realised, alternative, low cost, efficient and stable electrodes must be found to replace the expensive platinum-based electrocatalysts. It is therefore crucial for fuel cell development to explore more active and poison-resistant catalysts for the ORR that are superior in one, or preferably more, respects to the traditionally employed carbon-supported platinum (Pt/C) particle systems.

During the last decade a number of strategies have been proposed for enhancing the catalytic performance and at the same time minimizing Pt content. Substantial progress has been made through two families of catalysts. The first is described in Stamenkovic *et al*, Angew. Chem. Int. Ed., 2006, Sasaki *et al*, Angew. Chem. Int. Ed., 2010 and Kim *et al*, J. Am. Chem. Soc., 2010 and relates to the use of a Pt monolayer coated on non-noble fine particles (core shell structure) immobilized on an electrode. The second employs binary alloys of Pt in a general formula Pt_3M (M = Ni, Co, Fe, Ti, V, Pd, Mo, W, Cu, Ru) and is discussed in Stamenkovic *et al*, Science, 2007 and Lim *et al*, Science, 2009. Although these bimetallic catalysts have shown great improvements in activity, their structural complexity and the lack of procedures for controlled large-scale synthesis has limited their use in commercial devices. The exploration of non-noble metal compounds, notably cobalt- and iron-based nitrogen-containing catalysts (Lefevre *et al*, Science, 2009 and Zhang *et al*, Chem. Matter, 2009) are also promising substitutes for the currently used Pt/C catalyst owing to their comparable catalytic activities toward ORR and much lower cost.

A significant breakthrough was accomplished recently, when it was discovered that metal free nitrogen-doped vertically aligned carbon nanotubes can

not only match but actually surpass the performance of state-of-the-art Pt/C catalysts (Gong *et al*, Science, 2009). Gong *et al*, together with Qu *et al*, ACS Nano, 2010 and Liu *et al,* Angew. Chem. Int. Ed., 2010 reported similar improvements with other nitrogen doped nanocarbon materials such as nitrogen graphene and graphitic arrays. N-graphene and N-carbon nanotubes were clearly shown to catalyse a four-electron ORR process free from CO "poisoning" with a four or three fold higher electrocatalytic activity and better long term operational stability than that of commercially available Pt-based electrodes in alkaline electrolytes. Nevertheless, despite these emerging improvements in the activity of non metal catalysts, there is no clear understanding about the nature of the active sites and the mechanism that underpins the oxygen reduction reaction remains elusive. Very recently, other carbon materials doped with both lower electronegative atoms than carbon such as P-doped graphite layers (electronegativity of phosphorus: 2.19)[Liu, Z. W. et al. Angew. Chem., Int. Ed. 2011, 50, 3257–3261] and B-doped CNTs (electronegativity of boron: 2.04) [Yang, L.; et al. Angew. Chem., Int. Ed. 2011, 50, 7132–7135.] or of equal electronegative atoms such as sulphur doped[Zhi Yang, et al. ACS Nano, 2012, 6 , 205–211] or Iodine doped graphene (electronegativity of Iodine , Sulfur: 2.5)[Zhen Yao et al. Chem. Commun., 2012,48, 1027-1029,] have also shown pronounced catalytic activity.. So far, the catalytic activity has been attributed exclusively to the incorporation of heretoatoms in the graphene sheets and the resultant strong positive charge distribution around the carbon atoms, which leads to a significant improvement in the interaction between the carbon and oxygen molecules.

From a commercial point of view, the production of N-doped graphene reported so far is cumbersome and entails many steps. In general, N-doped graphene is produced by a chemical vapour deposition method that requires detachment from the substrate, purification in strong acids and subsequent doping in an ammonia atmosphere. Evidently, vapour deposition type processes are poorly suited for large scale production or for low cost manufacture. An alternative process that allows production of catalysts using facile methods is thus highly desirable for high volume production. Recently the metal free synthesis of N doped graphene through thermal

annealing of graphene oxide with melamine was reported.(Sheng, Z. H.; et al. ACS Nano 2011, 5, 4350–4358)

There remains, therefore, a need for new metal free catalyst systems which possess improvements in efficiency, poisoning resistance and/or stability or which can be made more cheaply, more easily and/or more quickly than those known in the art. Improvement in multiple factors is desirable. Ultimately, a viable commercial alternative to the platinum electrocatalysts currently used, which can be developed on a large scale and is poison resistant is desired. The present inventors have surprisingly established that catalysts comprising oxygen-doped graphene can address one or more of these issues and can exhibit excellent catalytic activity for the ORR. These catalysts include highly oxygenated graphenes such as graphene oxide and those with a lower atomic percentage oxygen, such as reduced graphene oxides.. Such oxygen doped graphene catalysts can show improved stability and/or poisoning resistance and hence represent promising alternatives to those already known in the art. In particular, the catalysts of the invention can possess excellent tolerance to the methanol crossover effect.

Summary of the Invention

The present invention relates to the development by the inventors of new catalyst materials, catalyst layers, fuel cells and methods for the use of these. Viewed from a first aspect the invention thus provides a catalyst for the oxygen reduction reaction at the cathode of a fuel cell, wherein the catalyst comprises oxygen-doped graphene. Preferably, the catalyst of the invention is metal-free.

Viewed from another aspect, the invention provides a catalyst as herein defined, wherein the oxygen-doped graphene is in the form of oxygen-doped graphene nanosheets or oxygen-doped graphene nanoflakes. The graphene nanoflakes are optionally and preferably vertically aligned (as defined herein).

Viewed from another aspect, the invention provides a catalyst layer comprising a catalyst as herein defined.

Viewed from another aspect, the invention provides an electrode comprising a catalyst layer as herein defined.

Viewed from another aspect, the invention provides a fuel cell comprising an electrode as herein defined. The fuel cell is preferably a proton exchange membrane fuel cell.

Viewed from another aspect, the invention provides a method of reducing oxygen, said method comprising exposing oxygen to a catalyst as herein defined. The method may correspondingly also be performed by exposing oxygen to the catalyst layer or electrode of the invention or by supplying oxygen to the cathode of the fuel cell of the invention.

Viewed from another aspect, the invention provides for the use of oxygen-doped graphene as a catalyst for the oxygen reduction reaction at the cathode of a fuel cell.

Detailed Description of the Invention

The present invention relates to catalysts, their products, uses, methods of formation and other aspects wherein a doped graphene is utilised. The term "graphene" is used herein to refer to a single atom thick planar sheet of sp^2-bonded carbon atoms which are positioned in a honeycomb crystal lattice. In the context of the present invention, the term "oxygen-doped graphene" is used to refer to graphene, onto which oxygen atoms have been chemically bound. This is particularly by means of at least one covalent bond such as one or more covalent single-bonds or a covalent double-bond. The oxygen can be in any chemical form, such as epoxy, hydroxy, carboxyl or carboxylic acid groups. The oxygen doping is preferably not solely in the form of adsorbed oxygen or oxygen held by non-bonded electrostatic interactions. Methods for the production of oxygen doped graphene are well known and documented in the art and are further described in the Examples herein.

The term "dopant" is used to describe an impurity element which is inserted into a substance in order to alter the properties of the substance. Oxygen doping of graphene is a key aspect of the present invention and oxygen doped graphene is intended herein in any instance where the dopant is not specified. Other doping or co-doping materials may also be used in addition to oxygen in all embodiments. Thus any oxygen doped graphene described herein may optionally also comprise at

least one additional dopant (co-dopant, additional dopant or second dopant). Each additional dopant may independently be added before, simultaneously with or after the oxygen dopant. Many of these other doping or co-doping materials are known in the art and some are indicated herein. Suitable co-doping materials include all dopants indicated herein such as nitrogen, chlorine and fluorine. Doping with one or more elements more electronegative than carbon is particularly desirable and thus co-doping with oxygen plus at least one additional dopant more electronegative than carbon forms a preferred embodiment.

Catalyst

The catalyst of the invention comprises, and optionally consists of, oxygen-doped graphene (with an optional co-dopant). The oxygen-doped graphene can take any form but is preferably in the form of oxygen-doped graphene nanosheets or oxygen-doped graphene nanoflakes. The oxygen doped graphene may optionally also be doped with other elements as indicated herein. The catalyst of the invention as indicated herein in all respects may be employed in any of the indicated forms in any aspect of the invention.

Where the graphene is in the form of nanoflakes, these may be positioned perpendicular to a surface in a formation often termed "vertically aligned". This term is used in the art and herein to indicate the position of nanoflakes such that one edge of each flake is against a surface. This may be the surface upon which the flakes were formed. An example of a suitable surface is a carbon surface, such as carbon clothpaper. In this context, the graphene nanoflakes referred to herein may be vertically aligned oxygen doped graphene nanoflakes (as defined herein). "vertically" as used herein does not imply any position relative to the ground or the action of gravity but rather that the nanoflakes are substantially perpendicular to a substrate such as the suitable surface described above. This is the conventional use of this term in the relevant art.

Where the graphene is in the form of nanosheets, these may comprise multiple layers. A preferred number of layers is in the range 1 to 10 (e.g 2 to 10) and more preferably 1 to 4 (e.g. 2 to 4).

The oxygen content of the oxygen-doped graphene in all embodiments herein is preferably in the range 3.8 to 40 atom% (e.g. 15 to 40 atomic %, such as 15 to 35 at%, more preferably 4 to 35 atom% (e.g. 20 to 35 atomic %, such as20 to 30 at%). In one embodiment, graphene oxide may be comprised in the oxygen-doped graphene and in that case the oxygen content will most commonly be 10 to 40 atom%, preferably 15 to 40 or 20 to 35 atom %. In an alternative embodiment, the oxygen-doped graphene may comprise at least one form of "reduced" graphene oxide, such as electrochemically reduced graphene oxide (ERGO) and/or nitrogen-reduced graphene oxide (NRGO). Where at least one reduced graphene oxide forms 50% or more of the oxygen-doped graphene, the oxygen content will typically be in the range of 3.5 to 25 at% (e.g. 3.8 to 25 at%), preferably 3.8 to 18 at% (e.g. 4 to 14 at%).

Upon reduction of GO (see Examples), the oxygen atomic concentration decreases from 27.7 at% in GO to 11.6at% in NRGO, (as experimentally determined in by the inventors) and to levels between 5-4 at% in ERGO according to the reported literature (see examples for citations). Graphene nanosheets produced by ionic liquid assisted grinding possess low levels of naturally absorbed oxygen (e.g. up to around 3.5 at%), inherited from the starting graphite. Such low oxygen level is very difficult to remove completely even with high temperature vacuum annealing at very high temperatures of 1000 °C.

It is important to appreciate that the oxygen-doped graphenes used in the present invention, such as GO and reduced GO, including NRGO and ERGO, differ from "graphene" in a number of ways. These include the oxygen content and bonding configurations of the remaining oxygen and also the surface area of the product.

The ORR activity of a graphene (produced by grinding) and ERGO electrodes is displayed in figure 18.

ERGO produced by electrochemical reduction of GO possess a high surface area which is evident by the large capacitive and Faraday loop in figure 1. Without being bound by theory, it is thought that the observed increase in current and onset potential observed for the ERGO can be attributed to the remnant structural defects induced by harsh oxidation of the GO and probably “wrinkles” induced by the

electrochemical removal of oxygen resulting in large surface area. Highly preferred oxygen-doped graphenes for use in the present invention thus include GO, and reduced GO, particularly NRGO and ERGO.

In all aspects of the invention, it is possible for the catalyst of the invention to further comprise a second, preferably non-metallic, heteroatom dopant. The second dopant is not oxygen and is referred to herein as a co-dopant, additional dopant or second dopant. Examples of second dopants include nitrogen, chlorine and fluorine. Nitrogen is particularly preferred as a second dopant. When nitrogen is present as an additional dopant, it is preferable that the nitrogen is covalently bound, such as by incorporation into the crystal lattice of the oxygen-doped graphene in substitutional (also known quartenary) or pyridine-like sites. Methods for the formation of nitrogen doped graphenes are known in the art. The second dopant may optionally be used in any aspect of the invention. More than one "second" dopant may be present. A suitable level of second or additional dopant will depend upon the nature of that dopant and the level of oxygen doping and any other dopants present. The total doping level will typically be 5 to 50 atomic % (e.g. 10 to 40 at% or 15 to 40 at%), more preferably 15 to 35 (e.g.10 to 35, 15 to 35 or 20 to 35 atomic %, such as 15 to 30 at% or 20 to 30 at%). Thus, an additional dopant may be present at levels of 0.1 to 40 at%, preferably 1 to 35 at%, more preferably 2 to 30 at% (e.g. 5 to 30, 2 to 10 or 5 to 15 at%). In one embodiment the level of oxygen doping (measured as atomic %) will be higher than the combined level of all other dopant materials.

Nitrogen reduced graphene oxide (NRGO) forms one preferred embodiment of the present invention and the oxygen doped graphene may thus consist in whole or in part (e.g. 2% to 99 (such as 2% to 20%)), or 2% to at least 11%) of NRGO. In one embodiment, the oxygen doped graphene comprises or consists of GO, NRGO, ERGO and mixtures thereof.

In all aspects of the invention, it is especially preferred if the catalyst is metal-free. This term is well understood in the art, but could be taken, for example, to mean that there is no metal present at a level greater than 1 at%, preferably no greater than 0.5 or 0.2 at%, and more preferably no greater than 0.1 or 0.01 at%. A level of 0.001 to 0.1 at% might be typical.

The catalyst of the invention can form part of cathode catalyst layer in the proton exchange membrane assembly in PEM fuel cells. Typically the catalyst, (e.g. graphene oxide and/or a reduced graphene oxide) has an average size (for example in the largest dimension) of 300 nm. The cathode will typically comprise oxygen doped graphene deposited on Toray paper. Such a catalyst layer will preferably be effective in the catalysis of the oxygen reduction reaction, particularly when exposed to oxygen, most preferably in a fuel cell.

Furthermore, the catalysts and catalyst layers of the invention may be used to coat an electrode. Any electrode is suitable, although preferable electrodes include glassy carbon electrodes, graphite felt and carbon fibers. Such an electrode will preferably be effective in generating charge by means of the oxygen reduction reaction, particularly when exposed to oxygen, most particularly in a fuel cell.

The catalyst of the invention is capable of catalysing the reduction of oxygen. The reduction of oxygen may be achieved by exposing oxygen to the catalysts, catalyst layers or electrodes of the invention as defined herein. The oxygen may be in any suitable form, such as pure oxygen gas or preferably as an oxygen-containing gas mixture, most preferably air (which may include dry or partially dried or treated air).

Specifically, the catalyst is effective for catalysing the oxygen reduction reaction at a cathode, particularly the cathode of a fuel cell. The method of the invention may therefore also be achieved by supplying oxygen (in any appropriate form) at the cathode of a fuel cell (such as a cathode and fuel cell as herein described).

Without being bound by theory, it is thought that the oxygen reduction reaction (ORR) which takes place at the cathode of a fuel cell can proceed *via* a four- or two-electron process. The four electron process involves the combination of oxygen with electrons and protons in a single step to produce water. The two-electron process consists of two steps; the first of these produces hydrogen peroxide ions as an intermediate and the second converts these to water.

In all embodiments, the catalysts of the invention may catalyse the ORR by any process and may catalyse (or be capable of catalysing) the ORR by a four-electron process. Thus, in the method of the invention, this will optionally be a

method for the reduction of oxygen by a four-electron process. Correspondingly, the catalysts, catalyst layers electrodes and fuel cells of the present invention may be used in the reduction of oxygen by a four-electron process.

Alternatively, where a GO or reduced graphene oxide, such as ERGO or NRGO is used, the ORR may take place by means of a two-electron process. All aspects of the invention will thus potentially be provided in the form of the four-electron reduction process and/or in the form of the two electron process with GO and/or reduced GO, such as ERGO and/or NRGO. Thus, in the method of the invention, this will optionally be a method for the reduction of oxygen by a two-electron process. Correspondingly, the catalysts, catalyst layers electrodes and fuel cells of the present invention may be used in the reduction of oxygen by a two-electron process.

One advantage of a two-electron process is that this may be used in the production of hydrogen peroxide from oxygen (e.g. atmospheric oxygen). Thus in a further embodiment, the present invention provides of the use of any of the oxygen doped graphenes, catalysts, catalyst layers or electrochemical cells in the production of hydrogen peroxide. Correspondingly, the invention provides for a method of the production of hydrogen peroxide comprising use of any or the materials or catalysts mentioned herein. Such a method will typically be an electrochemical method.

Fuel Cell

The catalysts, catalyst layers and electrodes of the invention may be incorporated into a fuel cell.

A fuel cell is an electrochemical cell which converts a source fuel and an oxidant (typically molecular oxygen) into an electric current. In its most basic form, a fuel cell comprises two electrodes, an anode and a cathode, each of which is in contact with at least one electrolyte. The electrolyte may be in solid or liquid form and can further comprise an ion-permeable membrane, such as a proton exchange membrane. The source fuel is supplied to the anode, where it is oxidised to form ions and electrons. The electrolyte allows the passage of ions (or of secondary ions). The electrons are forced to travel through an external circuit, generating the electric

current. Correspondingly, electrons and ions then recombine, together with another reagent, commonly oxygen, at the cathode to generate a product.

The fuel cells of the invention can be any known type of fuel cell in the art. A proton exchange membrane fuel cell is particularly preferred.

In all embodiments, example fuels which can be supplied to the anode of the fuel cells of the invention include hydrocarbon liquids or gasses, hydrogen gas, sugars, alcohols or mixtures thereof. Preferred fuels include light alcohols (e.g. C1 to C5 alcohols) such as ethanol or methanol, light hydrocarbons (such as C1 to C10 hydrocarbons), glucose, sucrose, hydrogen gas or mixtures thereof. Most preferred fuels include hydrogen gas and methanol.

In view of the above, the fuel cells of the invention, particularly when in use, may contain at least one fuel. Preferably this will be at least one fuel selected from ethanol, methanol, light hydrocarbons (such as C1 to C10 hydrocarbons), glucose, sucrose, hydrogen gas or mixtures thereof. Preferred fuels which may be present in the cell include hydrogen gas and methanol.

The fuel cells of the invention are suitable for use in a number of end applications, such as stationary or portable power sources, generation of current for electric vehicles, methods for allowing use of alternative fuels, such as in the transport industry, and portable charging for small electronic devices including, for example, phones (or other communication devices), cameras, music, game and/or video players (or other entertainment devices), navigation devices, prosthetic devices and/or portable computers.

Methods of Manufacture

The catalysts of the invention can be prepared by any method known in the art.

Here, highly oxidised Graphene Oxide (GO) was produced using a modified Hummer's process (.Eda, G.; Fanchini, G.; Chhowalla, M. *Nat. Nanotechnol.* **2008**, *3*, 270) The starting material Graphite powder (product: 78391) had a particle size $\leq$20 μm.

The vertically aligned multilayer graphene nanoflakes (MGNFs), which terminate on a few graphene layers (~2 nm thick edges) using microwave plasma enhanced chemical vapour deposition have been previously reported (Shang N.; Papakonstantinou, P.; etal , *Adv. Funct. Mater.*, **2008**, 18, 3506-3514) and can be grown directly on carbon paper (as shown in fig 9) or silicon substrate without the use of any metal catalyst. Oxygen/Nitrogen moieties can be introduced in graphene nanoflakes by treatment in acids and/or plasmas (e.g by treatment in plasmas induced by Electron cyclotron resonance as reported by Iyer, GRS, Papakonstantinou, P, Abbas, G, Maguire, PD and Bakirtzis, D (2009) *Dual Role of Purification and Functionalisation of Single Walled CNT by Electron Cyclotron Resonance (ECR) Nitrogen Plasma.* e-Journal of Surface Science and Nanotechnology, 7 . pp. 337-340. ISSN 1348-0391)

Figures

Figure 1. (a) TEM image of the triple-layered Graphene Oxide (GO) with the corresponding cross-sectional profile (bottom inset), and the SAED pattern (top inset). The arrows indicate the sheet separation (0.48 nm).

Figure 2. XRD spectra for pristine graphite and graphene oxide.

Figure 3. Raman spectra of GO compared to that of graphite

Figure 4. (a) Wide Energy Survey XPS Scan for GO and graphite; (b) Deconvoluted C1s spectra for GO.

Figure 5. (a) TGA and corresponding mass loss rate results for GO and pristine graphite. (b) Comparison of GO and Pt/C mass loss rate.

Figure 6. (a). Comparison of GO response in N_2 and O_2 , 0.1M KOH saturated solution. (b) Comparison of Pt/C response in N_2 and O_2 saturated solution

Figure 7. Comparison of the performance of traditional Pt/C cathode and Graphene oxide catalysts in the presence of methanol.

Figure 8. Stability (a) in sustained use and (b) in the presence of methanol of Pt/C and GO Pt/C catalysts.

Figure 9. CVs of pristine and oxygenated graphene nanoflakes in KOH saturated with N_2 and O_2 SEM images of graphene nanoflakes grown directly on carbon fibers.

Figure 10. Cyclic voltammograms taken at 1st, 7th, 22nd and 40th cycle of ERGO/GCE in 0.1M Na_2SO_4 aqueous solution. Scan rate: 50 mV/s

Figure 11. XPS spectra obtained from bulk samples of graphene oxide (GO) and Nitrogen doped reduced graphene oxide (NRGO)

Figure 12. Cyclic voltammetry curves of a) GO, b) ERGO electrodes in nitrogen (dotted curve)- and oxygen saturated (full curves) 0.1M KOH aqueous electrolyte solutions.

Figure 13. Linear-sweep voltammetry curves of bare GCE electrode compared with various GO mass loadings in oxygen saturated 0.1m KOH electrolyte at a scan rate of 10 mV/s and a rotation rate of 1600 rpm.

Figure 14. (a) CV curves of oxygen reduction on the GO, ERGO and NRGO electrodes in an O2-saturated 0.1M KOH solution at a scan rate of 100 mV/ s using a mass loading of 0.02mg; ERGOs have been subjected to 7 and 22 reducing cycles. (b) RDE curves for oxygen reduction on the GO, ERGOs, NRGO and Pt/C electrodes in an O2-saturated 0.1 M KOH solution at a scan rate of 10 mV /s.

Figure 15. (a) Rotating-disk voltammograms of ERGO (loading 0.28 mg/cm2) in O2-saturated 0.1 M KOH at a sweep rate of 10 mV/s and different rotation rates. (b) Corresponding Koutecky–Levich lot (I−1 vs. ω−0.5) at different potentials.

Figure 16. Polarization curves for ORR on commercial Pt/C (20 at%)catalyst in an O2-saturated 0.1 M KOH electrolyte containing 0, 0.1, 1, 2.5 and 5M methanol at a rotation rate of 1600 rpm and scan rate of 10 mV /s .

Figure 17. Polarization curves for ORR on ERGO electrode in an O_2-saturated 0.1 M KOH electrolyte containing 2.5 M methanol at a rotation rate of 1600 rpm and scan rate of 10 mV /s .

Figure 18. (a) CV curves of oxygen reduction on the graphene produced by ionic liquid assisted grinding and ERGO an O_2-saturated 0.1M KOH solution at a scan rate of 100 mV/ s using a mass loading of 0.02mg; ERGOs have been subjected to 22 reducing cycles. (b) RDE curves for oxygen reduction on the graphene and ERGO in O_2-saturated 0.1 M KOH solution at a scan rate of 10 mV /s.

Examples

1. Synthesis:

Highly oxidised GO was produced using a modified Hummer's process. Graphite (product: 78391) with particle size ≤ 20 μm was purchased from Fluka. All other chemical and reagents were purchased from Aldrich. A mixture of 2.5 g of Graphite and 1.9 g of $NaNO_3$ was placed in a flask cooled in an ice bath. 85 mL of H_2SO_4 was added to the mixture and stirred until homogenized. Solution of 11.25 g of $KMnO_4$ in distilled water was gradually added to the solution while stirring. After 2 hours, the solution was removed from the ice bath, and further stirred for 5 days. Brown-coloured viscous slurry was obtained. The slurry was added to 500 mL aqueous solution of 5 wt% H_2SO_4 over 1 hour while being continuously stirred. The

mixture was stirred for further 2 hours. After that, 10 ml of H_2O_2. (30 wt% aqueous solution) was added to the mixture and stirred for further 2 hours. This mixture was then left to settle overnight. The resultant mixture was filtered and further purified by dispersing in 500 mL aqueous solution of 3 wt% H_2SO_4 and 0.5 wt% H_2O_2. After two days of precipitation, supernatant solution was removed. This process was repeated five times. The solid obtained after the rigorous cleaning process was rinsed using copious amounts of distilled water and dried in oven, as reported in literature. Appropriate amounts of the solid was dispersed in water by ultrasonication for 2 h to produce a Graphene oxide aqueous dispersion.

Characterisation Techniques: Transmission electron microscopy (TEM) analyses were carried out using JEOL 2100F which has a point resolution of 0.19nm. TEM samples were prepared on Holey carbon-coated Cu 300 mesh grids. X-ray diffraction (XRD) data was collected using a Philips diffractometer 1050/81, employing a monochromatic Cu Kα radiation source (λ=1.54Å). Raman spectroscopy was performed using Argon laser (λ = 514.78nm) at ISA Lab-Raman system. For all spectroscopic studies, GO nanosheets were drop dried under infrared lamp to prepare thin films on Si substrates. XPS analysis was carried out using SCIENTA ECSA 300 equipped with monochromatic Al Kα (hυ =1486.6eV) X-ray source. Surface charging effect (due to insulating nature of as prepared GO) was neutralized using electron flood gun at 4.0eV.

Electrochemical Measurements. Cyclic voltammetry (CV) and chrono-amperometry (CA) measurements were performed with an AUTOLAB PGSTAT 20 potentiostat at room temperature. A conventional three-electrode cell was used with Ag/AgCl (saturated KCl) electrode, platinum wire, and a glassy carbon electrode (GCE, diameter: 3 mm) as reference, counter and working electrodes, respectively. Before each experiment, the GCE was polished by using 0.3 and 0.05 μm alumina powders followed by washing in ethanol and distilled water. Then, 20 μL aqueous solution of GO (0.5 mg/mL) was dropped on the GCE surface and dried under an infrared lamp.

2.1. Structural Characterization

2.1.1. High Resolution Transmission Electron Microscopy (HRTEM) of GO

HRTEM studies revealed the microscopic characteristics of as-prepared GO nanosheets, consisting of 2-4 layers, with limited sizes ranging from a few hundred nm to a couple of μm and a roughened surface due to the partial amorphous nature of the sample derived from the harsh oxidation steps involved in Hummer's method. Figure 1a exhibits a typical TEM image of the triple-layered GO with the cross-sectional profile (bottom inset of Fig. 1a). Despite the presence of such significant amount of O-species the long range orientational order is maintained. This is clear from the selected area electron diffraction (SAED) patterns (top inset of Fig. 1a), where triple layers exhibited three sets of diffraction points. The occurrence of these misoriented hexagonal patterns implies an incommensurate stacking of the GO sheets. This is not surprising as the functional groups protruding from the GO planes are expected to decouple the interactions between the carbon backbones of neighbouring layers.

2.1.2. X-ray Diffraction (XRD) of GO

Figure 2 shows XRD patterns of GO and graphite, for comparison purposes. The starting pristine graphite, PG, exhibits atomically flat pristine graphene sheets with a well-known van der Waals thickness of ~0.337 nm, estimated by using Bragg's equation for the (002) peak located at ~26.4°. The complete oxidation of GO was evidenced by the appearance of a new broad (002) peak (GO-peak) at $2\theta = 11.2°$ with 0.78 nm d-spacing, in place of the characteristic C(002) graphite peak ($2\theta = 26.4°$). The increased d-spacing of GO sheets is due to the presence of abundant O-moieties on both sides of the graphene sheet causing an atomic-scale roughness on the graphene sheet.

2.1.3. Raman Spectroscopy of GO

Raman spectroscopy is a powerful probe of both phonon dispersion and electron phonon coupling and serves as a sensitive probe of the extent of chemical modification of graphene. In Micro-Raman spectra (Fig. 3), the GO sample shows a

prominent D peak with intensity comparable to G peak in sharp contrast to the small D peak of PG, indicative of significant structural disorder due to the O-incorporation. The sharp increase in the D peak, suggesting increase in the in-plane disorder, leads to an increase in ID/IG ratio (from ~0.26 for PG to 0.93 for GO) and hence a decrease in in-plane crystal or domain size from ~17 nm (PG) to ~4.7 nm (GO). Steep decrease in intensity and broadening of the D′ peak for GO means loss of 3-D order along the crystallographic axis after oxidation. The G peak of GO is shifted to higher wavenumbers with respect to that of graphite. Similar upward shifting of the G band has been observed in heavily oxidised carbon nanotubes and is most likely related to the emergence of a Raman active band overlapped with G band. This band becomes active due to phonon confinement caused by the defects.

2.1.4. High Resolution X-ray Photoelectron Spectroscopy (XPS) of GO

High resolution C1s spectrum exhibited well-defined double peak formations, implicating extreme oxidisation of pristine GO (at RT, Fig. 4). The assignment of C1s components were based on theoretical predictions of core level shifts and on reported spectra containing the particular oxygen functional groups. In addition to the sp^2 graphite component at 284.49 eV, we found four broad components to account for the overlapping C1s features. The component at 285.86 eV is assigned to C atoms directly bonded to oxygen in hydroxyl configurations (shifts of 1–1.5 eV to higher BE). The component at 286.55 eV is attributed to epoxide group (C-O-C), and the smaller components at 287.54 and 288.94 eV are related to carbonyl (>C=O) and carboxyl groups (COOH or HO-C=O).

2.1.5. TGA analysis of GO and Pt/C

Figure 5a shows the residual mass percentage and differential curves as a function of temperature of pristine graphite as GO, obtained from TGA analysis. The GO starts to lose mass upon heating even below 100 °C, which is associated with elimination of loosely bound or adsorbed water and gas molecules. First major mass loss can be observed along with an exothermic signal of mass loss rate (dW/dT, I)

around 200 °C, presumably due to reduction of the edge-plane O-moieties, yielding CO, CO_2, and steam as by-products of the reduction process. Second the largest mass loss, and corresponding exothermic dW/dT signal, starts at Tr > 300 °C & continues till 600 °C, (II, Fig. 5a). No residue was found in these three samples. In figure 5b the GO sample is compared with Pt/CB which showed a residual Pt of 21.65%

2.2. Electrochemical Analysis

2.2.1 Cyclic Voltammetry

For the ORR measurements, the as-synthesized GO and commercial Pt/C (20 wt% Pt) were coated onto a glassy carbon (GC) electrode by drop drying under an infra red lamp. Figure 6a compares the CVs for GO in N_2 and O_2 saturated 0.1 M KOH solution. The GO shows a substantial reduction process at about -0.3 V in the presence of oxygen, while no obvious response was observed at the same potential range under N_2. Owing to the nitrogen and metal-free synthesis of GO the observed electrocatalytic activity toward the ORR is attributed exclusively to the presence of oxygen groups in the graphene structure.

Specific current response for Pt/C in N_2 and O_2 saturated KOH solution are compared in figure 6b. The current response of Pt/C (60 μA) for ORR is slightly higher than that of GO (53 μA). Since Pt/CB already shows the H_2 adsorption/desorption peak in the same region as ORR it is essential to subtract the effect to properly identify the correct ORR response of Pt/CB. As such peak heights were calculated and the effect of previously existing H_2 adsorption/desorption peak was subtracted. The values thus obtained (Table 2) confirm that GO actually shows a better ORR response (53.3% higher peak height) than Pt/CB.

Table 2.

Sample	Vp(V)	ORR peak height(μA)
GO	-0.290	52.9
Pt/C	-0.16	34.5

We have also investigated the electrochemical stability of the GO electrode for the ORR in O_2-saturated 0.1 M KOH solution in the presence of 2M methanol using cyclic voltammetry (Figure 7). As expected due the response of Pt/CB changes drastically in the presence of methanol ; the ORR peak vanishes whereas the methanol oxidation peak appears in the forward scan followed by a poisonous peak (resultant of residual carbonaceous species) during the reverse CV scan. On the contrary no significant change is observed for GO indicating significant tolerance for methanol poisoning.

2.2.2. Chrono-amperometeric Studies.

We have also investigated the electrochemical stability of the GO electrode for the ORR in O_2-saturated 0.1 M KOH solution for 6000 seconds using cyclic voltammetry. Current response of GO and Pt/C electrodes over time was measured as a percentage of their respective initial current value. Both electrodes exhibited an initial loss followed by a more stable behaviour upon further cycling. However significant initial current loss was observed for the Pt/C electrocatalyst compared to much smaller loss exhibited by GO indicating that the catalytic sites of the GO are rather stable in a basic medium.

Figure 8 compares the specific current response for GO and Pt/CB in the presence of 2M methanol introduced after 1000s of the initial scan time. Due to the oxidation of methanol a sudden jump in the current is observed upon introduction of methanol in Pt/C. The behaviour of GO was observed to be fairly independent of the presence of methanol. It exhibited a small initial (negative) increase in current and quickly regained its stable performance.

3. - Reduced GO

In order to study the role of oxygen groups on the electrocatalytic activity of graphene oxide, one would require pure graphene oxide in colloidal form with progressively reduced amounts of oxygen down to zero. The oxygen groups of

graphene oxide can be progressively reduced by hydrazine-solution based treatment. However this leads to the simultaneous formation of nitrogen-functional groups and incomplete elimination of oxygen groups, along with issues associated with the inherent toxicity of hydrazine. On the other hand, thermal annealing of graphene oxide at high temperatures although more efficient, is not compatible with deposition on glassy carbon electrode, (GGE) electrode. To overcome these deficiencies, an electrochemical reduction process has been adopted here to convert GO to electrochemically reduced GO (ERGO).

3.1 - Experimental procedures

Synthesis of GO and Electrochemically reduced GO(ERGO)

The graphene oxide was synthesized from natural graphite powder based on the Hummers method. The electrochemical reduction of GO experiment was carried out in N_2 saturated 0.1 M Na_2SO_4 in the potential range 0 to –1.5 V (vs. Ag/AgCl) at a scan rate of 50 mV/s for up to 40 cycles to obtain ERGO/GCE. Alternative electrochemical reduction procedures are also effective on reducing GO (Peng, X. Y.; Liu, X. X.; Diamond, D.; Lau, K. T.; " Synthesis of electrochemically-reduced graphene oxide film with controllable size and thickness and its use in supercapacitor", Carbon, 2011, 49. 3488-3496) .

3.1.1 –Synthesis of NRGO

Nitrogen doped Reduced Graphene Oxide (NrGO) prepared by a hydrothermal approach was used for comparison purposes. Briefly 50 mg of Graphite oxide was dispersed in 40ml of DI water and exfoliated by ultrasonication for 60min. In a typical the GO solution was mixed with 50µl of ammonia (28% wt in H_2O, Sigma Aldrich) and 700µl of hydrazine (35% wt in H_2O, Sigma Aldrich). The weight ratio of hydrazine to GO was 50:10. The mixture was stirred for 15min and transferred to 200ml of Teflon lined vessel for hydrothermal reaction at 160C for three hours. The resultant product was cleaned with DI water and NrGO was collected by centrifuging at 5000rpm for 30min.

3.1.2 – Electrode preparation and Catalyst deposition

The preparation method of the working electrodes containing investigated catalysts (GO, ERGO and NrGO) is as follows. Glassy carbon electrode (GCE) was polished with alumina powders, then rinsed thoroughly, and finally dried with blowing N_2. In short, 5 mg of catalyst powder was dispersed in 1 ml of DMF mixed solvent with 50 µl of Nafion solution (5 wt%, Sigma-Aldrich), then the mixture was ultrasonicated for at least 60min to generate a homogeneous ink. Next, a 4 µL portion of 5mg/ml catalyst suspension was spread on a pretreated bare GCE using a micropipet tip, leading to the catalyst loading 0.28 mg /cm^2. Finally, the as-prepared catalyst film was dried at room temperature. For comparison, bare glassy carbon electrode, which has been polished and cleaned was also dried for electrochemical measurement. Before the electrochemical measurement, the electrolyte (0.1 M KOH) was degassed by bubbling oxygen for 30 min. The polarization curves were obtained by sweeping the potential from 0.2 to -1 V vs. Ag/AgCl at room temperature and 1600 rpm, with a sweep rate of 10 mV/ s. All the data were recorded after applying a number of potential sweeps until which were stable.

3.1.3 - Electrochemical reduction of GO

The electrochemical reduction experiment was carried out in N_2 saturated 0.1 M Na_2SO_4 in the potential range 0 to –1.5 V (vs. Ag/AgCl) at a scan rate of 50 mV/s for up to 40 cycles to obtain ERGO/GCE.

The cyclic voltammograms (Figure 10) of a GO modified glassy carbon electrode (GCE) in a potential range from 0.0 to -1.5 V shows a large cathodic current peak at 1.5 V with a starting potential of -0.9 V. This large reduction current should be due to the reduction of the surface oxygen groups since the reduction of water to hydrogen occurs at more negative potentials (e.g., 1.5 V). In the second cycle, the reduction current at negative potentials decreases considerably and almost disappears after ~20 potential scans. This demonstrates that the reduction of surface-oxygenated species at GO occurs quickly and irreversibly and the exfoliated GO could be reduced electrochemically at negative potentials.

3.2 - Composition of GO and NRGO

The elemental compositions (table) and nitrogen –bonding configurations (Figure 11) in nitrogen doped reduced graphene oxide (NRGO) and graphene oxide were investigated using X-ray photoelectron spectroscopy (XPS). The oxygen atomic concentration was decreased from 27.7 at% in GO to 11.6at% in NrGO, (as experimentally determined in our lab) and to levels between 5-4 at% in ERGO according to the reported literature (Peng, Carbon, 2011, Zhou, M.et al. "Controlled Synthesis of Large-Area and Patterned Electrochemically Reduced graphene oxide films" Chem. Eur. J. 2009, 15, 6116 – 6120). It should be mentioned that graphene nanosheets produced by ionic liquid assisted grinding possess low levels of naturally absorbed oxygen (~3.5 at%), inherited from the starting graphite (Shang, N. et al. "Controllable selective exfoliation of high-quality graphene nanosheets and nanodots by ionic liquid assisted grinding". Chem. Comm., 48, (2012) 1877-1879). Such low oxygen level is very difficult to be removed completely even with high temperature vacuum annealing at very high temperatures of 1000 C. The level of oxygen in ERGO is slightly more than from exfoliated graphene. The oxygen level in graphene is about ~3 at%.

Upon hydrothermal treatment of GO, the C1s spectrum exhibits a transformation from a double peak, characteristic of graphene oxide to a single sharp peak indicative of a trend to restore the sp2 bonding graphene character The wide X ray spectrum of NRGO shows clearly the presence of nitrogen . The N 1s peak can be deconvoluted into two sub-peaks at 399.0 and 400.5 eV, which have been assigned to pyridinc and pyrrolic N in the film. A doping level of 6.25 at% nitrogen in the NrGO was obtained and the N binding configuration includes 55 % pyridinic N, 45% pyrrolic N.

Table : chemical composition of grapgene oxide (GO) and N-doped reduced graphene oxide (NRGO)

Sample	**O (at%)**	**C (at%)**	**N (at%)**
Graphene oxide GO	27.72	72.28	0
N-doped reduced graphene oxide NRGO	11.64	82.11	6.25

3.3 - Cyclic Voltammetry ORR performance in N_2 and O_2 saturated alkaline solution

To investigate the electrocatalytic activity of the ERGO for the ORR we compared its electrocatalytic properties with those of GO and nitrogen doped reduced graphene oxide (NRGO) by cyclic voltammetry in an aqueous solution of nitrogen and O_2-saturated, 0.1M KOH solution at a scanning rate of 10 mV/s. GO showed a substantial reduction process in the presence of oxygen, whereas no obvious response was observed under nitrogen (Figure 12). The onset and peak potentials of ORR on the ERGO and NRGO electrodes are more positive, and their current densities much higher, than those on the GO electrode, implying that reduction and heteroatom doping with N effectively improved the ORR activity.

Comparison between the three electrodes shows that reduction of GO through either electrochemical or through hydrothermal approaches causes substantial increase on the background current. This finding strongly indicates that the partial removal of oxygen functionalities by either electrochemical reduction process or hydrothermal assisted chemical method had similar impact on the electronic structure of graphene.

3.4 - Effect of GO loading on ORR performance

To gain an insight into the role of the GO catalyst during the ORR electrochemical process we investigated its electrocatalytic performance as a function of mass loading. We carried out CVs and the linear sweep voltammetric (LSV) measurements on a rotating disk electrode (RDE) with GO loadings varying from 5 to 40 μg on a GCE in an O_2-saturated 0.1 M KOH electrolyte solution. GO shows a similar LSV profile to GCE, but with a more positive onset potential and higher current density, and hence an overall better ORR activity. All five loading showed a substantial reduction process in the presence of oxygen, whereas no obvious response was observed under nitrogen. As shown in Figure 13 the onset and peak potentials of ORR did not show any substantial change with mass loading, however a systematic decrease on current density was observed consistent with the insulating nature of GO. As shown in Figure 13, the typical two-step pathway was observed for the GO electrode with onset potentials at around -0.28 and -0.65 V, indicating a

successive two-electron reaction pathway, instead of the direct four-electron pathway seen for the commercial Pt/C electrode.

Such ORR on set potentials correspond to two separate reduction processes via the following equations:

$$O_2 + 2H_2O + 2e^- \rightarrow 4HO_2^{\square} + OH^-$$

$$HO_2^{\square}{}_{\square} + H_2O + 2e^- \rightarrow 3OH^-$$

Since GO is an insulator the active sites facilitating ORR on GO are limited to narrow zones of the electrode electrolyte three-phase boundaries (TPB) because of the poor ET efficiency, which leads to a less than optimal ORR performance. One effective way to increase the Electron transfer efficiency is to increase the electron-conductivity of the materials by a reduction process.

3.5 – Comparison of ORR performance of GO, ERGO and NrGO

The electrocatalytic activities of the GO/GCE and ERGO/GCE electrodes were evaluated by CV and RDE voltammetries. A catalyst with a higher electrocatalytic activity toward the ORR will demonstrate an earlier onset potential and a higher peak current. Accordingly, its RDE voltammogram should also show a sooner current drop with a positively shifted onset potential and a higher steady-state current.

The cyclic voltammograms (CVs) of electrochemically reduced GO together with those of NRGO and Pt/C for oxygen reduction at a constant active mass loading (0.02 mg; except for Pt/C which is 0.01mg) in an aqueous O_2-saturated 0.1 M KOH solution are shown in Figure 14a. As can be seen, the onset potential of ORR for the GO electrode subjected to 22 reducing cycles is at -0.18V (versus AgCl) with the cathodic reduction peak around -0.40V (versus AgCl). Upon electrochemical reduction of graphene oxide both the onset potential and the ORR reduction peak potential shifted positively to -0.11 V and -0.26 V respectively, accompanied by a concomitant increase in the peak current density (Figure 14a). These results clearly

demonstrated a significant enhancement in the ORR electrocatalytic activity for the ERGO in respect to the graphene oxide electrode. Compared with GO, the ERGOs show dramatically increased capacitance, this is mainly related to increased conductivity of the material. The change in shape of the CV curves demonstrates the increase of non-Faradaic currents induced by the increase in effective surface area of electrically conductive graphene that are generated by reduction of GO.

To further investigate the ORR performance, we carried out the linear sweep voltammetric (LSV) measurements on a rotating disk electrode. As shown in Figure 14b, the ORR at the GO electrode commenced around -0.18 V (onset potential), whereas the ORR onset potential at the ERGO electrode subjected to 22 reducing cycles significantly shifted positively to -0.11 V with the limiting diffusion current at -1 V being about 1.7 times higher than that of the GO electrode. The electrocatalytic activity of ERGO graphene toward ORR in terms of the onset potential and current density is significant but not quite as good as that of the commercial Pt/C electrocatalyst (Figure 14b). The other advantages of the doped graphene catalysts, such as methanol tolerance, however are significant. Although the ORR electrocatalytic activity of the as-prepared ERGO electrode is still lower than that of a commercial Pt/C electrode, it is comparable to those of N-containing CNT-based graphene-based metal-free electrocatalysts, indicating the great catalytic ability of ERGO.

As shown in Figure 15 the electron transfer number (n) was calculated to be 2-2.8 at 0.6-0.8 V from the slopes of Koutecky_Levich plots suggesting ErGO favours a 2e oxygen reduction process in agreement with the peak observed on the LSV measurements in the region 06-0.8V(Figure 14b) .

3.6 - Methanol poisoning of Pt/C and ERGO

To examine the possible crossover effect in the presence of other fuel molecules (e.g., methanol) linear sweep voltammetric responses for ORR at the ERGO and Pt/C electrodes were obtained. As shown in Figure 16, for the commercial Pt/C catalyst, a sharp increase in the onset ORR potential was observed in the presence of methanol even at a very low concentration of 0.1M. However, the corresponding

onset potential for the ERGO electrode remained almost unchanged with a small decrease in the current density even after the addition of 2.5M methanol (figure 17). The results unambiguously show that the ERGO has much better methanol tolerance than the commercial Pt/C catalyst

5

Claims

1. A catalyst for the oxygen reduction reaction at the cathode of a cell such as a fuel cell, said catalyst comprising oxygen-doped graphene.

2. A catalyst as claimed in claim 1, wherein the graphene is in the form of oxygen-doped graphene nanosheets or oxygen-doped graphene nanoflakes.

3. A catalyst as claimed in either claim 1 or claim 2, wherein the oxygen-doped graphene nanosheets comprise multiple layers.

4. A catalyst as claimed in claim 3, wherein the number of layers is in the range 2 to 10.

5. A catalyst as claimed in any of claims 1 to 4, further comprising a second, non-metallic heteroatom dopant, which is not oxygen.

6. A catalyst as claimed in claim 5, wherein the second heteroatom is nitrogen.

7. A catalyst as claimed in claim 6, wherein the nitrogen dopant is incorporated into the crystal lattice of the graphene.

8. A catalyst as claimed in any of claims 1 to 7, wherein the catalyst is metal-free.

9. A catalyst as claimed in any preceding claim wherein the catalyst comprises graphene oxide, nitrogen reduced graphene oxide and/or electrochemically reduced graphene oxide.

10. A catalyst layer comprising the catalyst as claimed in any of claims 1 to 9.

11. An electrode comprising the catalyst layer of claim 10

12. A fuel cell comprising the electrode of claim 11.

13. A fuel cell as claimed in claim 12, wherein the fuel cell is a proton exchange membrane fuel cell.

14. A fuel cell as claimed in either claim 12 or claim 13, wherein the fuel supplied to the anode is selected from hydrogen gas and methanol.

15. A method of reducing oxygen, said method comprising exposing oxygen to the catalyst of any of claims 1 to 9.

16. A method as claimed in claim 15, wherein the method comprises exposing oxygen to the catalyst layer of claim 10.

17. A method as claimed in claim 15, wherein the method comprises exposing oxygen to the electrode of claim 11.

18. A method as claimed in claim 15, wherein the oxygen is supplied at the cathode of a fuel cell as defined in any of claims 12 to 14.

19. Use of oxygen-doped graphene as a catalyst for an oxygen reduction reaction.

20. Use as claimed in claim 19, wherein the catalyst is as defined in any of claims 1 to 9.

21. Use as claimed in claim 19 or claim 20 for the oxygen reduction reaction at the cathode of a fuel cell.

22 Use as claimed in claim 19 or claim 20 for the production of hydrogen peroxide.

23. Use as claimed in claim 21, wherein the fuel cell comprises a catalyst layer as defined in claim 10.

24. Use as claimed in claims 21 or 23, wherein the fuel cell comprises an electrode as defined in claim 11.

25. Use as claimed in claims 21 or 23, wherein the fuel cell is defined as in any of claims 12 to 14.

26 A method for the production of hydrogen peroxide comprising the exposing a catalyst as defined in any of claims 1 to 17 to oxygen.

Abstract

The present invention relates to a catalyst for the oxygen reduction reaction such as at the cathode of a fuel cell, a metal/air battery or in the generation of hydrogen peroxide. In particular to catalysts comprising oxygen-doped graphene such as graphene oxide and/or reduced graphene oxide. This invention is also directed to a catalyst layer comprising such a catalyst, an electrode comprising such a catalyst layer, a fuel cell comprising such an electrode and the use of said catalysts in the catalytic reduction of oxygen at the cathode of fuel cells.

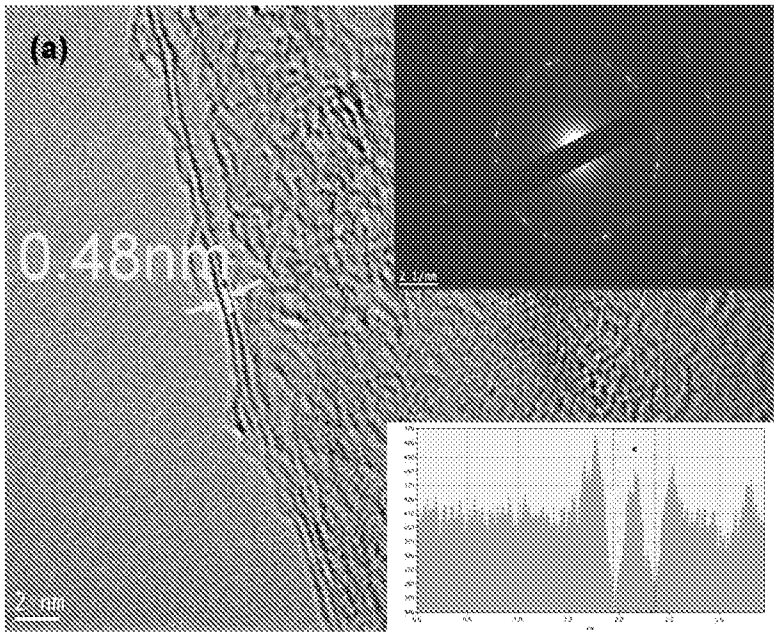

Figure 1. (a) TEM image of the triple-layered Graphene Oxide (GO) with the corresponding cross-sectional profile (bottom inset), and the SAED pattern (top inset). The arrows indicate the sheet separation (0.48 nm).

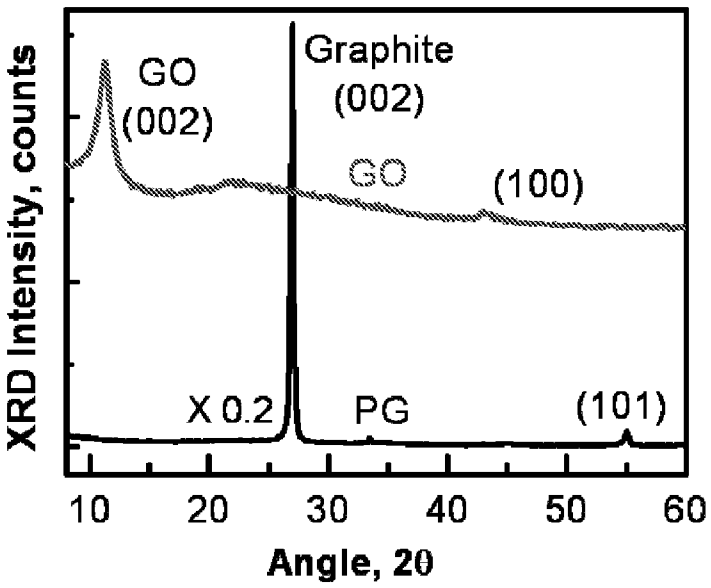

Figure 2. XRD spectra for pristine graphite and graphene oxide.

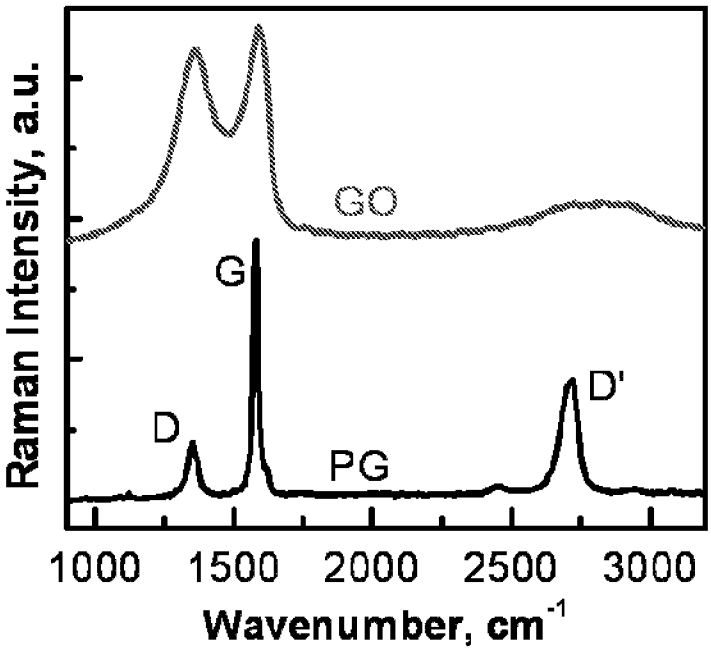

Figure 3. Raman spectra of GO compared to that of graphite

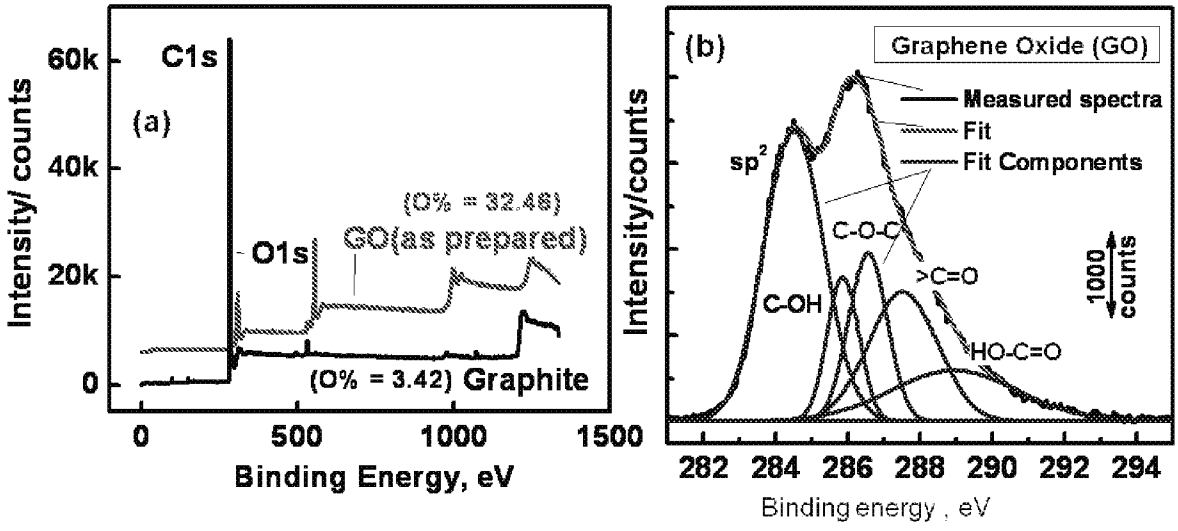

Figure 4 (a) Wide Energy Survey XPS Scan for GO and graphite; (b) Deconvoluted C1s spectra for GO .

a)

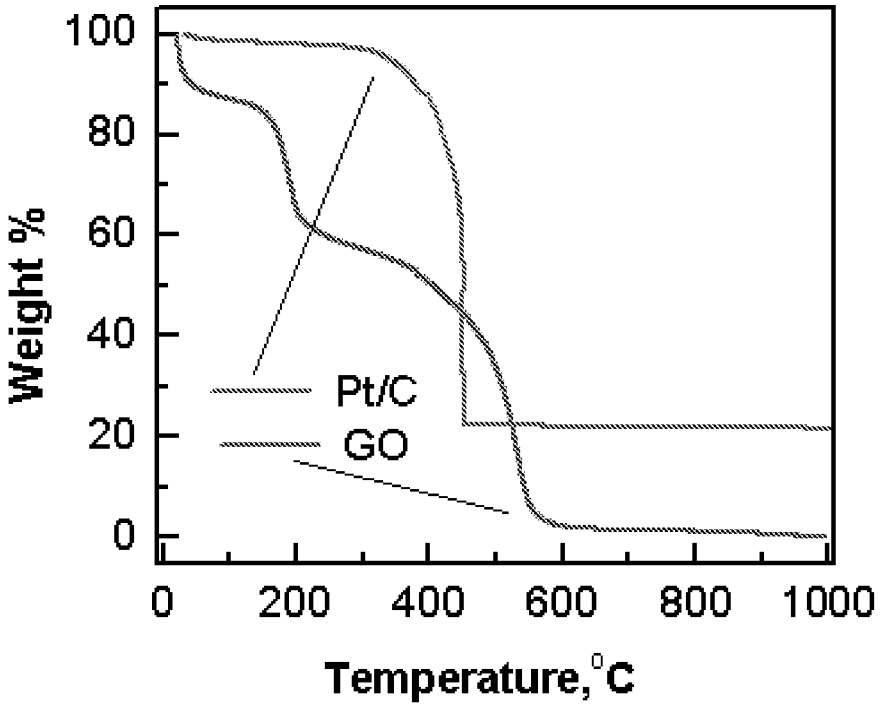

b)

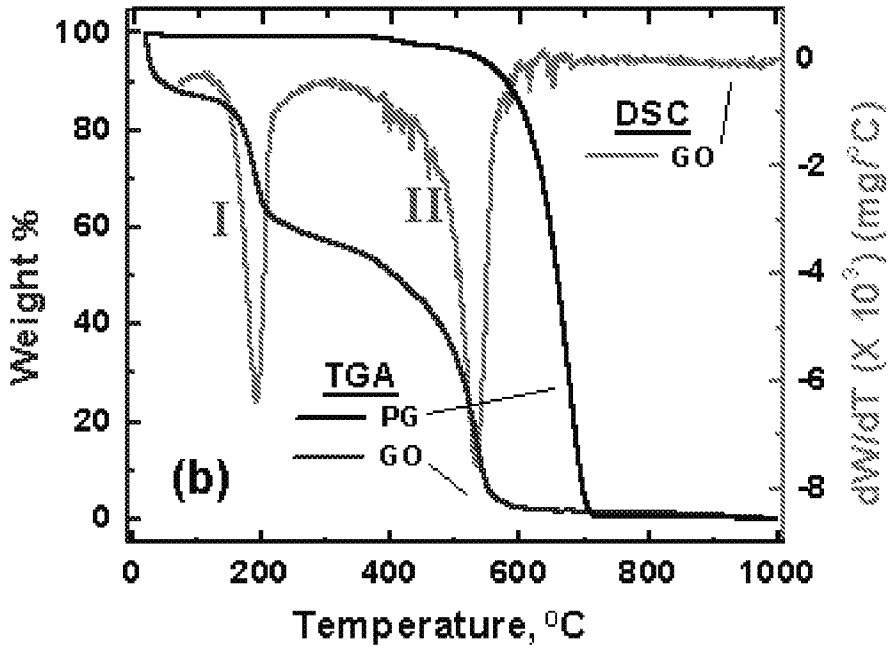

Figure 5. (a) Comparison of GO and Pt/C mass loss rate.

(b) TGA and corresponding mass loss rate results for GO and pristine graphite.

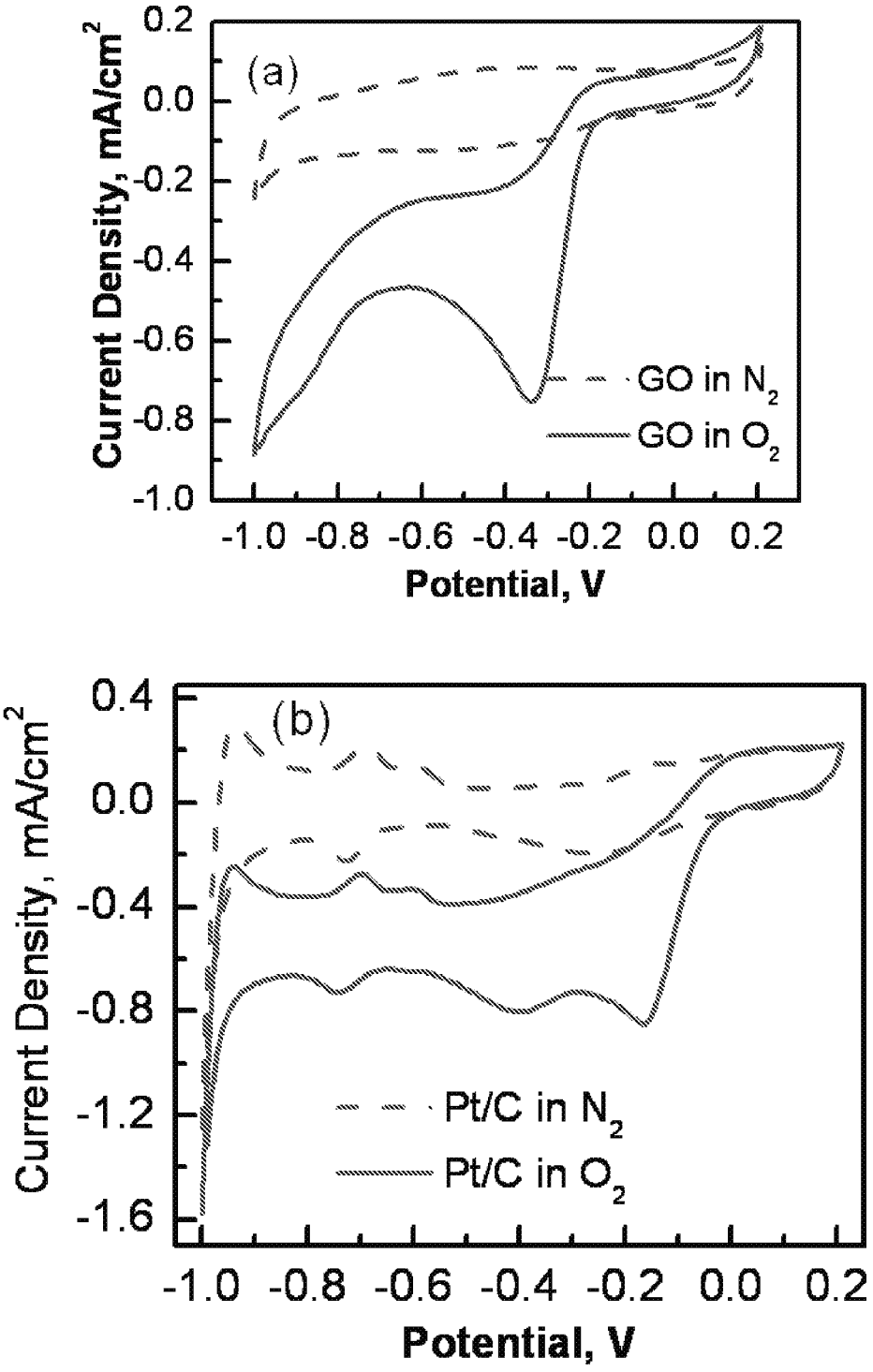

Figure 6(a). Comparison of cyclic voltammetric response of GO in N_2 and O_2 saturated solution. (b) Comparison of Pt/C response in N_2 and O_2 saturated solution

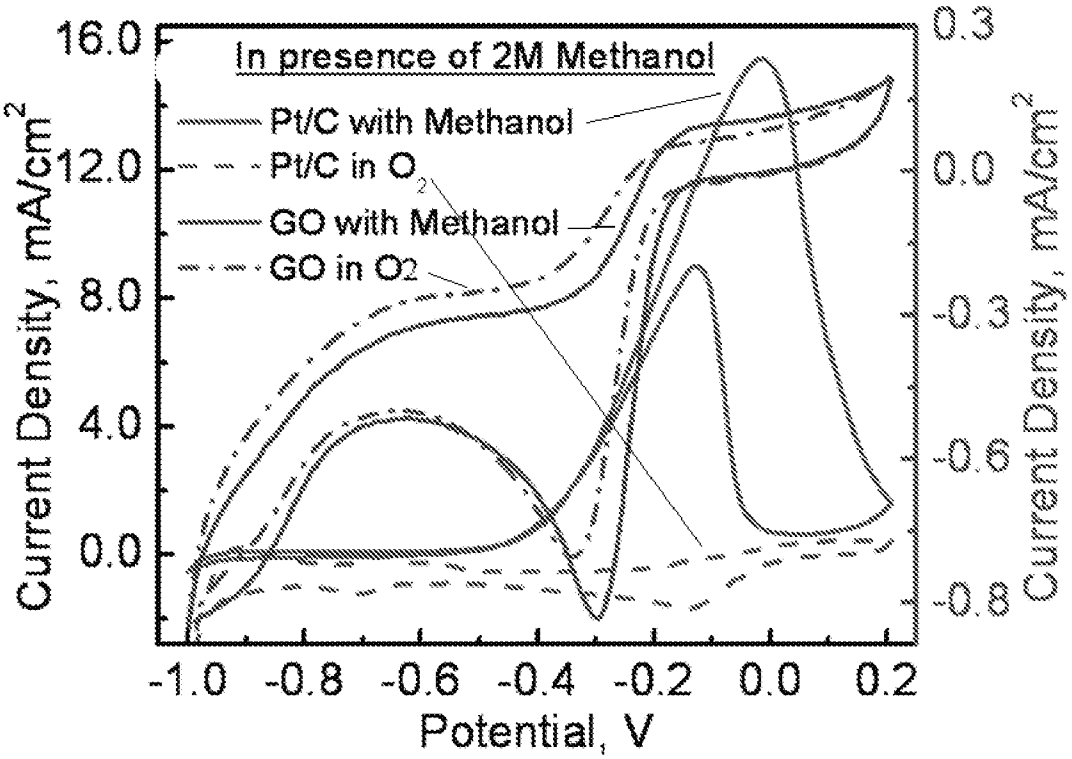

Figure 7. Comparison of cyclic voltammetric response of GO and Pt/C in O_2 saturated solutions and in the presence of 2 M methanol.

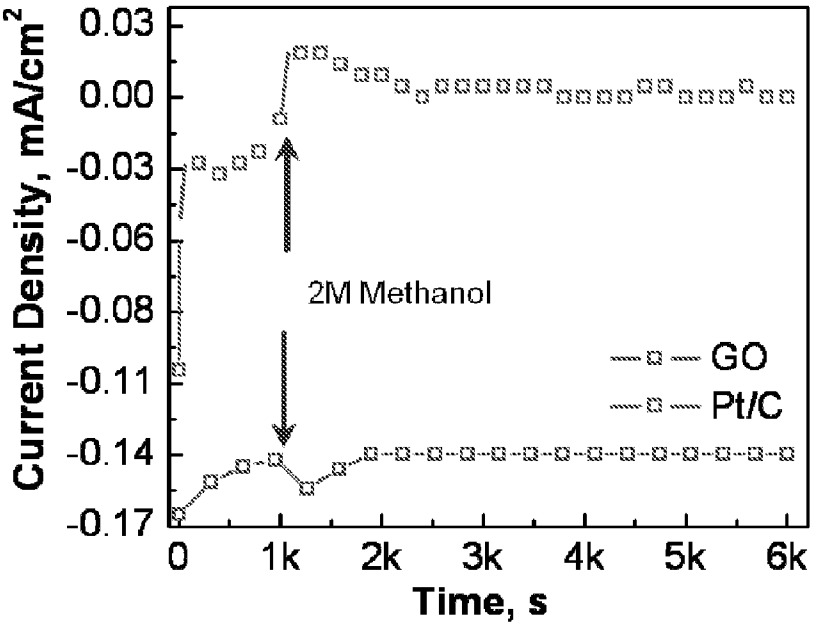

Figure 8: Chrono-amperometric studies for samples performed in O_2 saturated 0.1 M KOH solution at individual onset potentials.

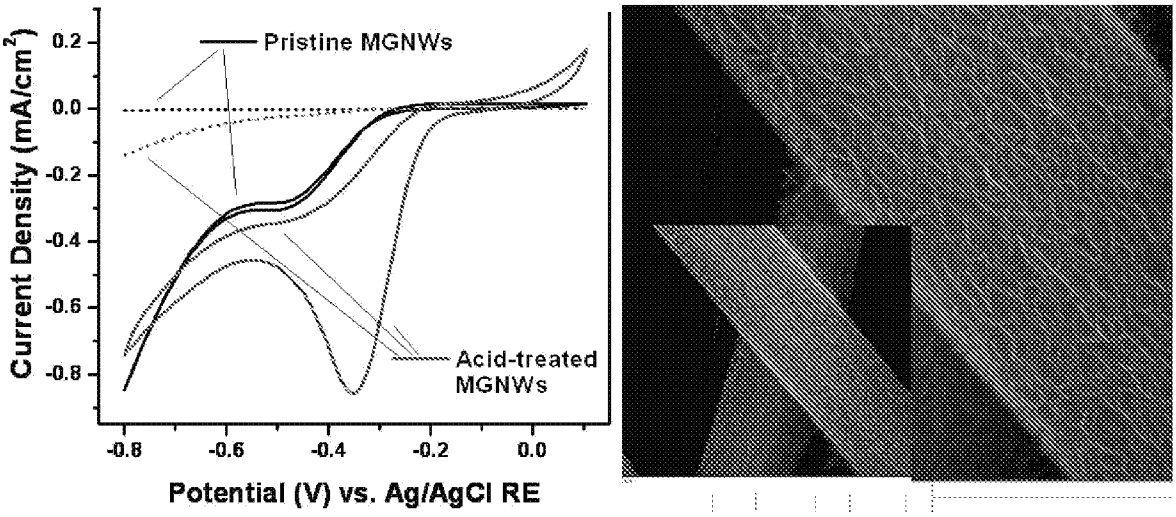

Figure 9: CVs of pristine and oxygenated graphene nanoflakes in KOH saturated with N_2 and O_2 SEM images of graphene nanoflakes grown directly on carbon fibers.

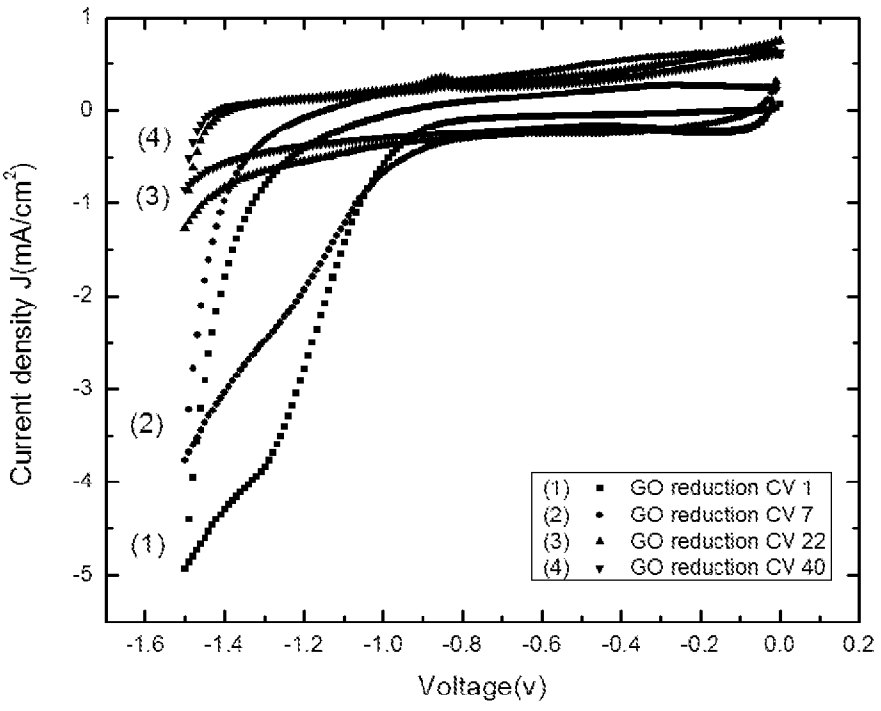

Figure 10. *Cyclic voltammograms taken at 1st, 7th, 22nd and 40th cycle of ERGO/GCE*

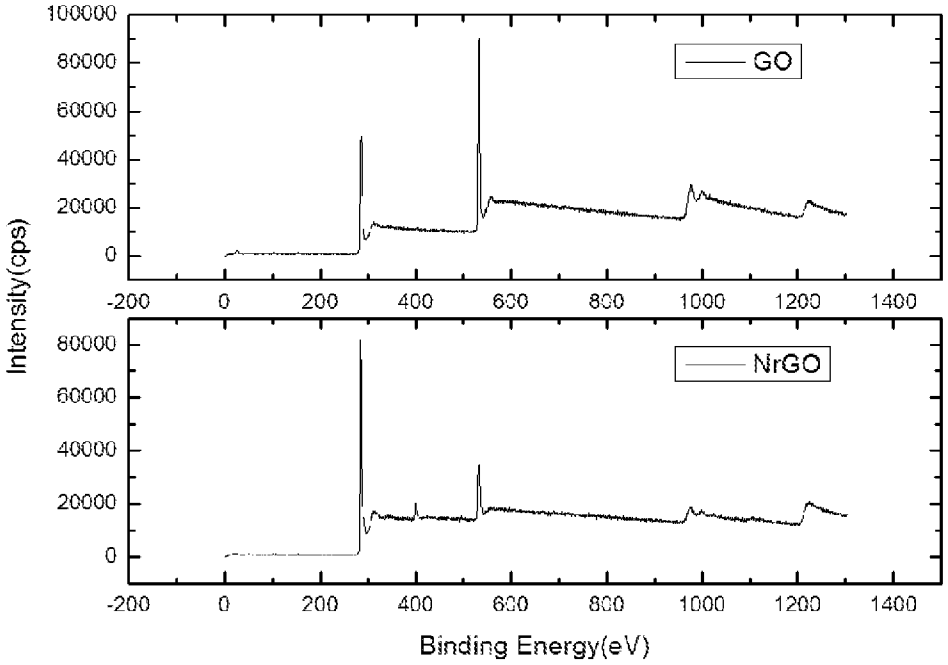

a)

Figure 11 *XPS spectra obtained from bulk samples of graphene oxide (GO) and Nitrogen doped reduced grapgene oxide (NrGO).*

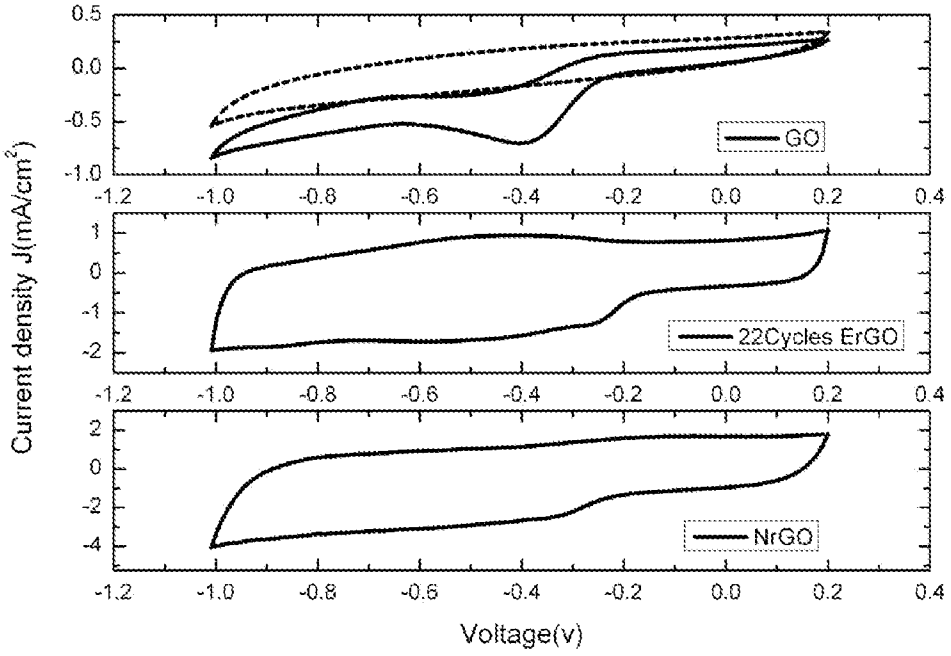

Figure 12. *Cyclic voltammetry curves of a) GO, b) ErGO electrodes in nitrogen (dotted curve)- and oxygen saturated (full curves).*

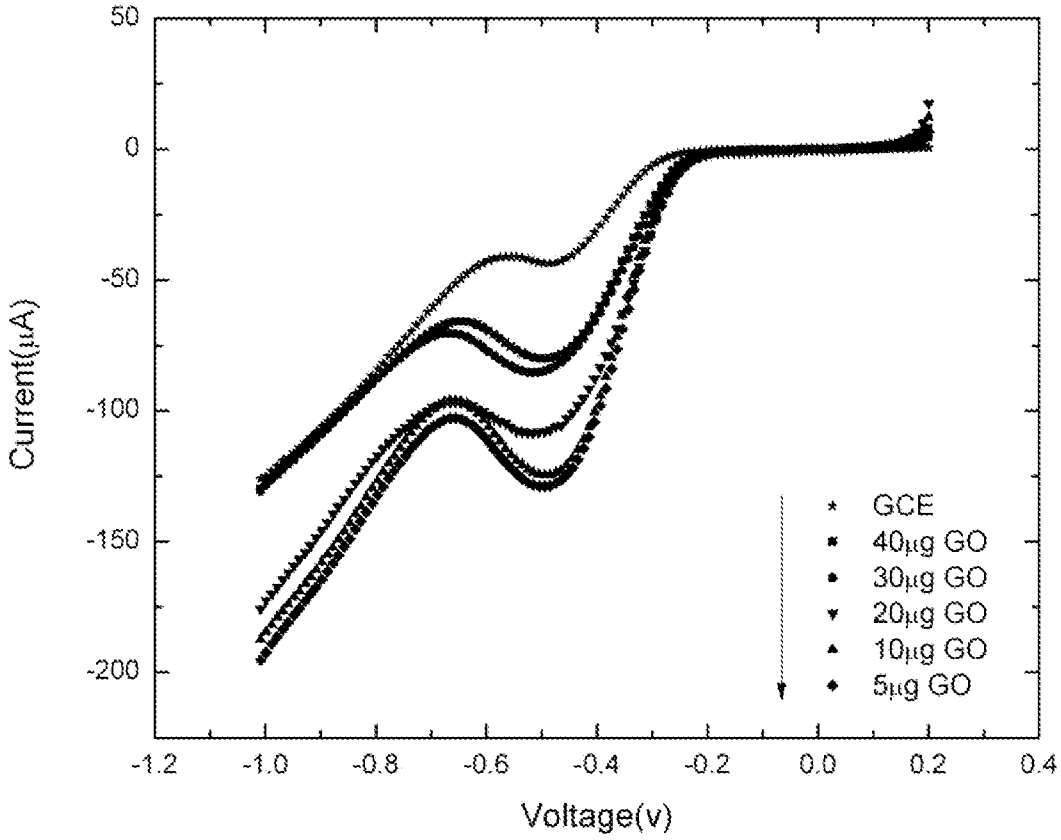

Figure 13. *Linear-sweep voltammetry curves of bare GCE electrode compared with various GO mass (in O_2).*

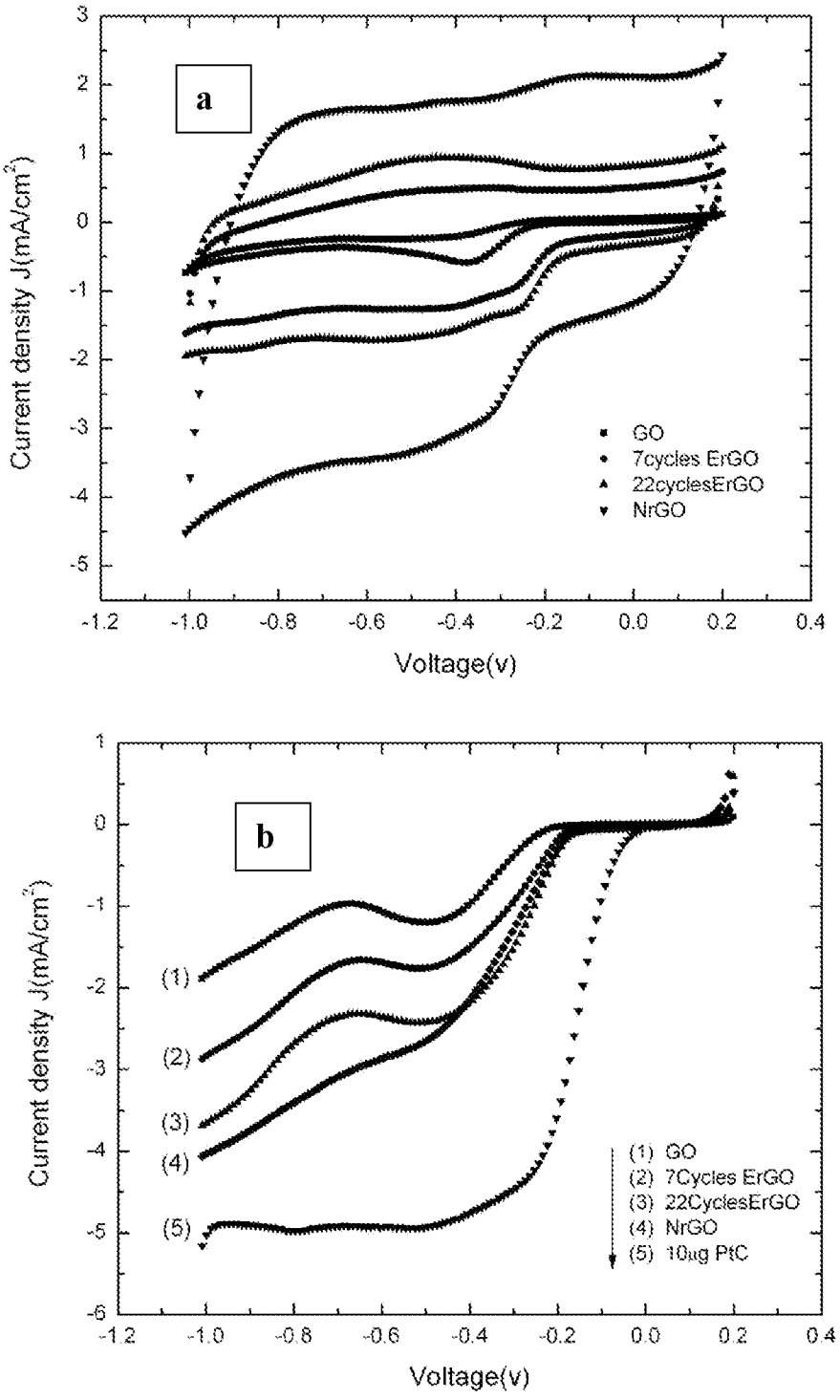

Figure 14. *(a) CV curves of oxygen reduction on the GO, ErGO and NrGO electrodes (b) RDE curves for oxygen reduction on the GO, ERGOs, NrGO and Pt/C electrodes.*

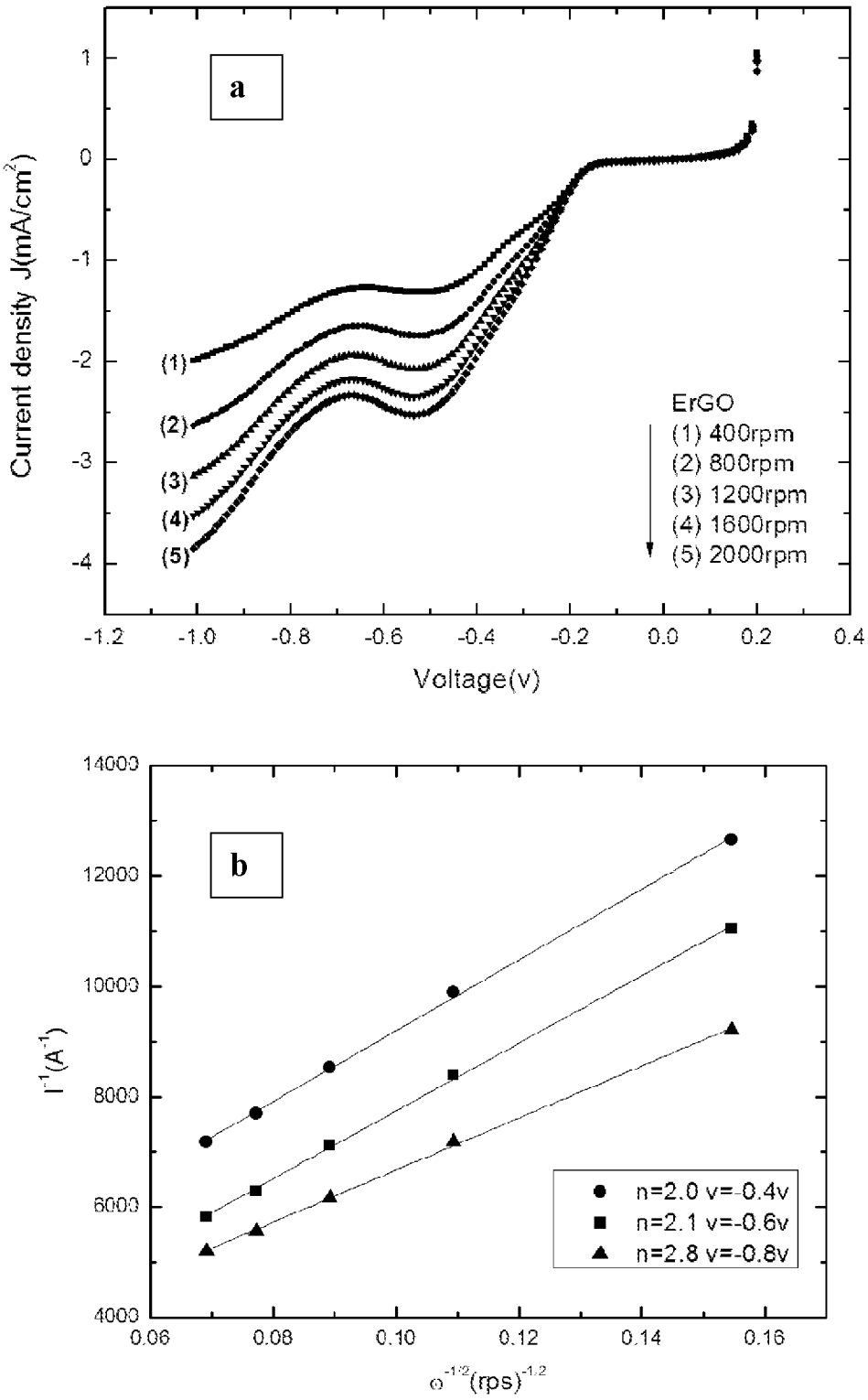

Figure 15. *(a)* Rotating-disk voltammograms of ERGO at different rotation rates. (b) Corresponding Koutecky–Levich lot (I^{-1} vs. $\omega^{-0.5}$) at different potentials.

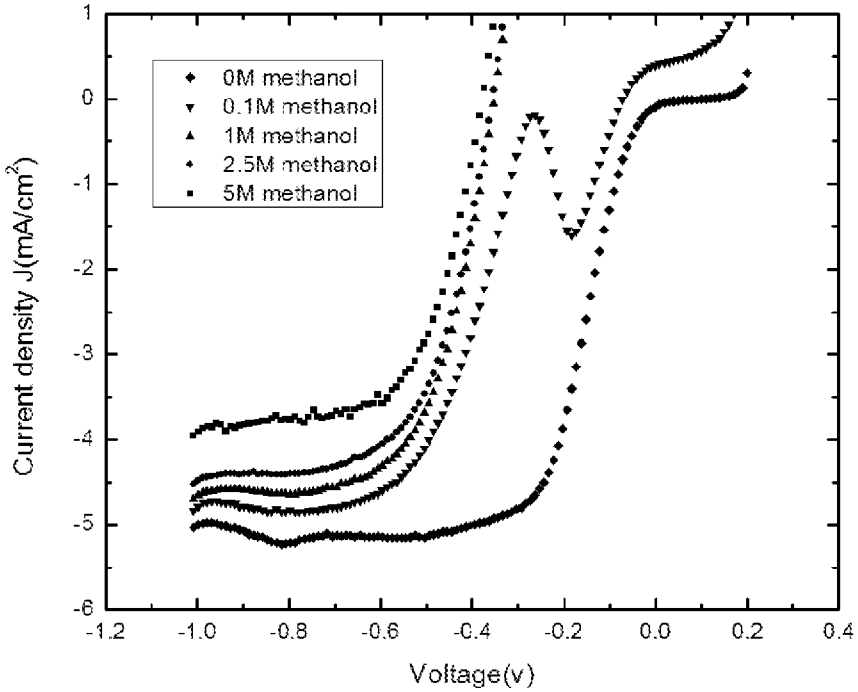

Figure 16 *Polarization curves for ORR on commercial Pt/C (20at%) with 0, 0.1, 1, 2.5 and 5M methanol .*

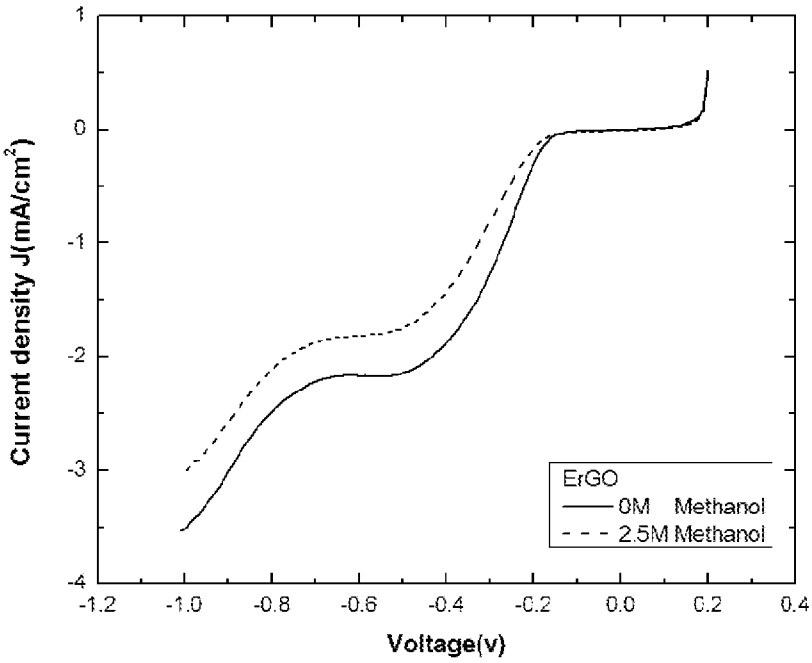

Figure 17 *Polarization curves for ORR on ERGO with* 2.5 M methanol.

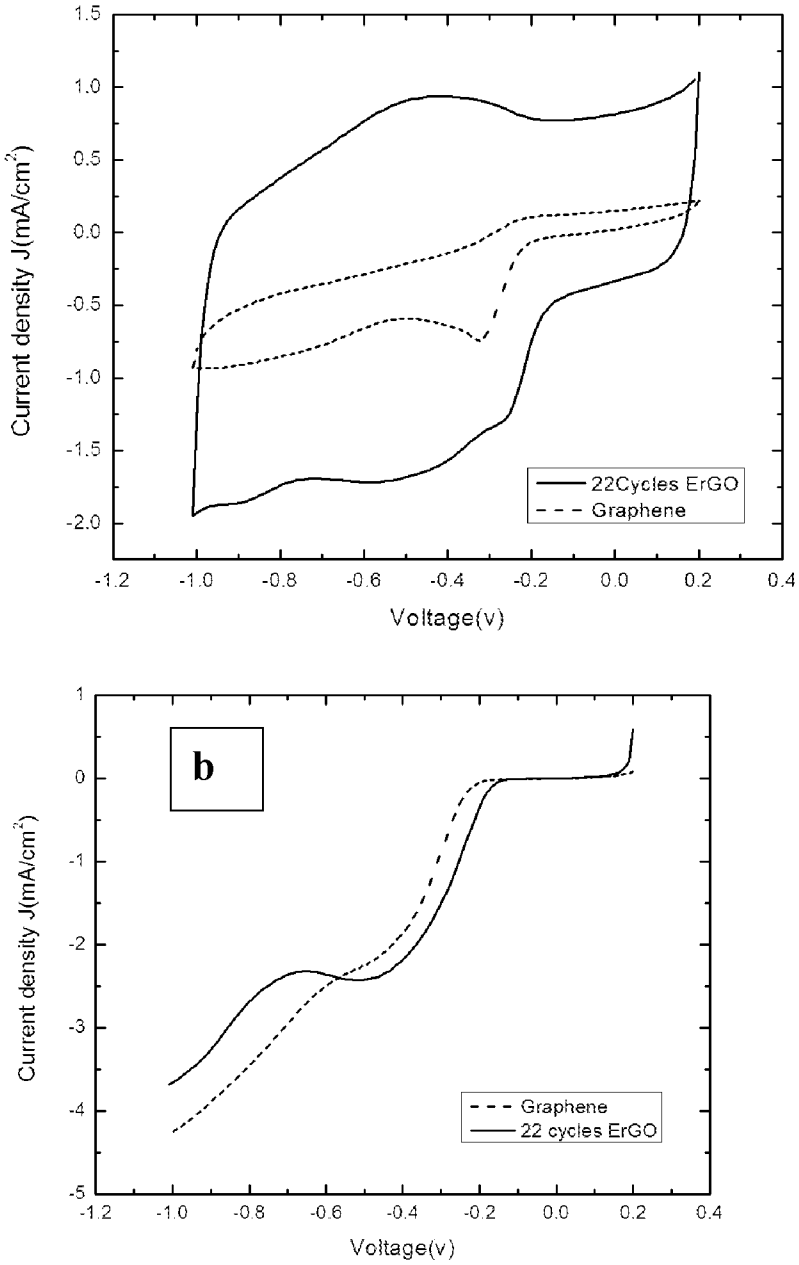

Figure 18. *(a) CV curves of oxygen reduction on graphene and ErGO (b) RDE curves for oxygen reduction on the graphene and ERGO in O_2-saturated 0.1 M KOH.*